

유연 뼈대 구조물의 비탄성 좌굴 해석

Inelastic Buckling Analysis of Partially Restrained Frame

김 승 억*
Kim Seung-Eock

김 문 겸**
Kim Moon Kyum

요 지

본 논문에서는 유연 연결부를 갖고 있는 이차원 구조물의 비탄성 좌굴해석을 연구하였다. 본 해석을 통하여 구조물의 기하학적, 및 재료적 비선형 뿐만 아니라 유연 연결부의 비선형 효과가 구조물의 거동과 강도에 미치는 영향을 예측할 수 있다. 본 해석 결과는 실험 결과와 비교하였으며 예제해석도 수행하였다.

1. INTRODUCTION

Conventional analysis and design of steel framed structures are usually carried out under the assumption that the beam-to-column connections are either fully rigid or ideally pinned. However, most connections used in current practice are partially restrained type whose behavior lies between these two extreme cases. The partially restrained connections influence the moment distribution in beams and columns as well as the drift ($P-\Delta$ effect) of the frame. One way to account for all these effects in partially restrained frame design is through the use of a direct inelastic buckling analysis. Since the power of personal computers and engineering workstations is rapidly increasing, it is feasible to employ inelastic buckling analysis directly in engineering design office. Herein, we shall develop an inelastic buckling analysis method for planar partially restrained frames.

Since the study is limited to two-dimensional steel frames, the spatial behavior of frames is not considered and lateral torsional buckling of members is assumed to be prevented by adequate lateral braces. This study covers both braced as well as unbraced partially restrained frames. A compact W-section is assumed so that the section can develop full plastic moment capacity without local buckling.

2. INELASTIC BUCKLING ANALYSIS OF PARTIALLY RESTRAINED FRAMES

The important attributes which affect the behavior of partially restrained frames may be grouped into three categories: geometric; material; and connection nonlinearities. The geometric nonlinearity includes second-order effects associated with the $P-\delta$ and $P-\Delta$ effects and geometric imperfections. The material nonlinearity includes gradual yielding associated with the influence of residual stresses and flexure behavior. The connection nonlinearity indicates the nonlinear

* 연세 대학교 토목공학과 Post Doc.

** 연세 대학교 토목공학과 교수

moment-rotation relationship of partially restrained connections.

2.1 Geometric Nonlinearity

The bending moments in a beam-column consist of two types: primary bending moment; and secondary bending moment. Primary bending moments are caused by applied end moments and/or transverse loads on members. Secondary bending moments are from axial compressive force acting through the lateral displacements of a member. The secondary bending moments include the $P-\delta$ and $P-\Delta$ moments. Herein, stability functions are used for each member to capture these second-order effects in a direct manner. The benefit of using stability functions is that it enables only one or two elements to predict accurately the second-order effect of each framed member [1].

2.2 Geometric Imperfection

Geometric imperfections result from unavoidable tolerance during fabrication or erection, and they may be classified as out-of-straightness and out-of-plumbness. These imperfections cause additional moments in column members. In this paper, geometric imperfections will be considered by an explicit imperfection modeling.

The AISC Code of Standard Practice limits an erection out-of-plumbness equal to $L_c/500$ in any story and no more than 2" of accumulated imperfection [2]. In this study, however, $L_c/500$ is used for all stories and this will be conservative because it will exceed the 2" accumulated limitation. The uniform imperfection may be easily implemented in practical design use, and the system strength is often governed by a weak story which has the out-of-plumbness equal to $L_c/500$.

The frame out-of-plumbness may be used for unbraced frames but not for braced frames. This is because the $P\Delta$ effect caused by out-of-plumbness is diminished by braces in braced frames. As a result, the member out-of-straightness instead of the out-of-plumbness must be used to account for geometric imperfections for braced frames. The AISC Code recommends a maximum fabrication tolerance of $L_c/1000$ for member out-of-straightness. In this study, the same geometric imperfection of $L_c/1000$ is adopted by the calibration with the plastic-zone solutions. The out-of-straightness may be assumed to vary sinusoidally with a maximum in-plane deflection of $L_c/1000$ at the mid-height. Ideally, many elements are necessary in order to model the sinusoidal out-of-straightness of a beam-column member. Two elements with a maximum deflection at the mid-height of a member are practically adequate to capture the imperfection effects [1].

2.3 Material Nonlinearity Associated with Residual Stress

Residual stresses result in a gradual axial stiffness degradation. The fibers that have the highest compressive residual stress will yield first under compressive force, followed by the fibers with a lower value of compressive residual stress. Due to this spread of yielding or plasticity, the axial and bending stiffnesses of a column segment are degraded gradually along the member. This stiffness degradation effect will be accounted for by the CRC tangent modulus concept as [3]:

$$E_t = 1.0E \quad \text{for } P \leq 0.5P_y \quad (1a)$$

$$E_t = 4 \frac{P}{P_y} E \left(1 - \frac{P}{P_y} \right) \quad \text{for } P > 0.5P_y \quad (1b)$$

where E_t = CRC tangent modulus, E = Young's modulus, P = axial force, and P_y = squash load.

2.4 Material Nonlinearity Associated with Flexure

When a wide flange section is subjected to pure bending, the moment-curvature relationship of a section has a smooth transition from elastic to fully plastic. This is because the section yields gradually from extreme fibers which have higher stresses than interior fibers. The gradual yielding effect leads to the concept of a softening plastic hinge which may be represented simply by a parabolic stiffness reduction function of a plastic hinge written as [4]:

$$\begin{bmatrix} \dot{M}_A \\ \dot{M}_B \\ \dot{P} \end{bmatrix} = \frac{E_t I}{L} \begin{bmatrix} \eta_A [S_1 - \frac{S_2^2}{S_1} (1 - \eta_B)] & \eta_A \eta_B S_2 & 0 \\ \eta_A \eta_B S_2 & \eta_B [S_1 - \frac{S_2^2}{S_1} (1 - \eta_A)] & 0 \\ 0 & 0 & A/I \end{bmatrix} \begin{bmatrix} \dot{\theta}_A \\ \dot{\theta}_B \\ \dot{e} \end{bmatrix} \quad (2)$$

where $\dot{M}_A, \dot{M}_B, \dot{P}$ = incremental end moments and axial force, respectively, S_1, S_2 = stability functions, E_t = tangent modulus, I = moment of inertia of cross section, L = length of element, A = area of cross section, η_A, η_B = scalar parameter for gradual inelastic stiffness reduction [4], $\dot{\theta}_A, \dot{\theta}_B$ = incremental rotations at element ends A and B, and \dot{e} = incremental axial deformation.

2.5 Connection Nonlinearity

The connection behavior is represented by its moment-rotation relationship. Extensive experimental works on connections have been performed, and a large body of moment-rotation data has been collected. Using these abundant data base, researchers have developed several connection models including: linear; polynomial; B-spline; power; and exponential models. Herein, the three-parameter power model proposed by Kishi and Chen is adopted [5]. The Kishi-Chen power model contains three parameters: initial connection stiffness R_{ki} , ultimate connection moment capacity M_u , and shape parameter n . The power model may be written as (Fig. 1):

$$m = \frac{\theta}{(1 + \theta^n)^{1/n}} \quad \text{for } \theta > 0, \quad m > 0 \quad (3)$$

where $m = M/M_u$, $\theta = \theta_r/\theta_o$, θ_o = reference plastic rotation, M_u/R_{ki} , M_u = ultimate moment capacity of the connection, R_{ki} = initial connection stiffness, and n = shape parameter. When the connection is loaded, the connection tangent stiffness R_{kt} at an arbitrary rotation θ_r can be derived by simply differentiating Eq. (3) as:

$$R_{kt} = \frac{dM}{d|\theta_r|} = \frac{M_u}{\theta_o(1-\theta^n)^{1+1/n}} \quad (4)$$

When the connection is unloaded, the tangent stiffness is equal to the initial stiffness as:

$$R_{kt} = \frac{dM}{d|\theta_r|} = \frac{M_u}{\theta_o} = R_{ki} \quad (5)$$

It is observed that a small value of the power index n makes a smooth transition curve from the initial stiffness R_{ki} to the ultimate moment M_u . On the contrary, a large value of the index n makes the transition more abruptly. In the extreme case, when n is infinity, the curve becomes a bilinear line consisting of the initial stiffness R_{ki} and the ultimate moment capacity M_u .

An important task for practical use of the power model is to determine the three parameters for a given connection configuration. The practical procedures for determining the three parameters are presented in Ref. [1] for the following four types of connections with angles: single/double web-angle connections; and top- and seat-angle with/without double web-angle connections.

Figure 2 shows a beam-column element with partially restrained connections at both ends. If the effect of connection flexibility is incorporated into the member stiffness, the incremental element force-displacement relationship of Eq. (2) is modified as [4]:

$$\begin{bmatrix} \dot{M}_A \\ \dot{M}_B \\ \dot{P} \end{bmatrix} = \frac{EJ}{L} \begin{bmatrix} S_{ii}^* & S_{ij}^* & 0 \\ S_{ij}^* & S_{jj}^* & 0 \\ 0 & 0 & A/I \end{bmatrix} \begin{bmatrix} \dot{\theta}_A \\ \dot{\theta}_B \\ \dot{e} \end{bmatrix} \quad (6)$$

where

$$S_{ii}^* = (S_{ij} + \frac{EJ S_{ii} S_{jj}}{LR_{ktB}} - \frac{EJ S_{ij}^2}{LR_{ktB}}) / R^* \quad (7a)$$

$$S_{jj}^* = (S_{ij} + \frac{EJ S_{ii} S_{jj}}{LR_{ktA}} - \frac{EJ S_{ij}^2}{LR_{ktA}}) / R^* \quad (7b)$$

$$S_{ij}^* = S_{ij} / R^* \quad (7c)$$

$$R^* = \left(1 + \frac{E I S_{ii}}{L R_{kiA}}\right) \left(1 + \frac{E I S_{jj}}{L R_{kiB}}\right) - \left(\frac{E I}{L}\right)^2 \frac{S_{ij}^2}{R_{kiA} R_{kiB}} \quad (7d)$$

where R_{kiA} , R_{kiB} = tangent stiffness of connections A and B, S_{ii} , S_{ij} = generalized stability functions, and S_{ii}^* , S_{ij}^* = modified stability functions that account for the presence of end connections. The tangent stiffness (R_{kiA} , R_{kiB}) accounts for the different types of partially restrained connections (see Eq. (4)).

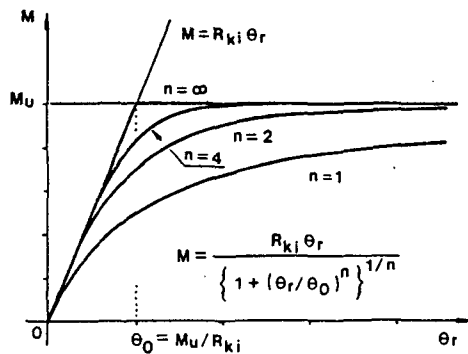


Fig. 1. Moment-Rotation Behavior of Three-Parameter Model

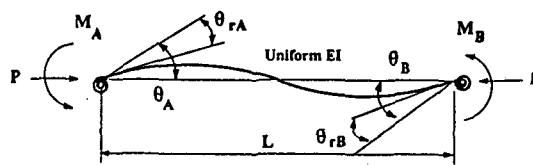


Fig. 2. Beam-Column Element with Semi-Rigid Connections

3. VERIFICATION STUDY

In the open literature, no benchmark problems solving partially restrained frames with geometric imperfections are available for a verification study. An alternative is to separate the effects of partially restrained connections and geometric imperfections.

3.1 Effect of Partially Restrained Connections

Stelmack studied the experimental response of two flexibly-connected steel frames [6]. A two-story, one-bay frame in his study is selected as a benchmark for the present study. The frame was fabricated from A36 W5×16 sections, with pinned base supports (Fig. 3). The connections were bolted top and seat angles ($L4 \times 4 \times 1/2$) made of A36 steel and A325

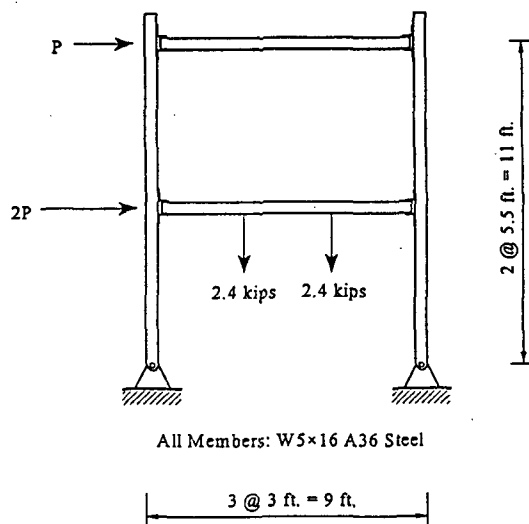


Fig. 3. Configuration and Load Condition of Stelmack's Two-Story Semi-Rigid Frame

3/4"D bolts. The experimental moment-rotation relationship is shown in Fig. 4. A gravity load of 2.4 kips was applied at third points along the beam at the first level, followed by a lateral load application. The lateral load-displacement relationship was provided in Stelmack's.

Herein, the three parameters of the power model are determined by curve-fitting and Eqs. in Ref. [1]. The three parameters obtained by the curve-fit are $R_{ki} = 40,000$ kip-in/rad., $M_u = 220$ kip-in, and $n = 0.91$. The parameters by the equations are $R_{ki} = 29,855$ kips/rad., $M_u = 185$ kip-in, and $n = 1.646$.

The moment-rotation curve given by experiment compares well with curve-fitting, and show some deviation with the equations (Fig. 4). In spite of this difference, the equations are a more practical alternative in design since experimental moment-rotation curves are not usually available. In the analysis, the gravity load is first applied, then the lateral load. The lateral displacements given by the proposed methods and by the experiment compare well up to the load given by the experiment (Fig. 5). The proposed method adequately predicts the behavior and strength of partially restrained connections.

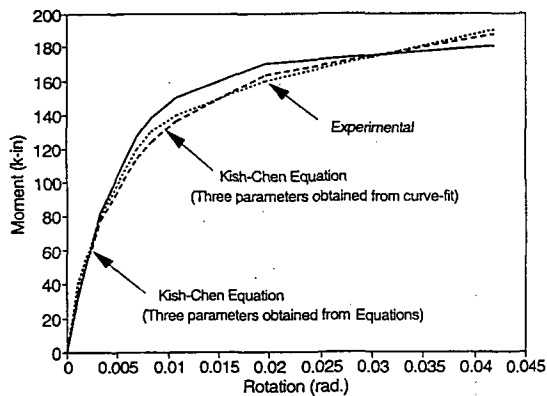


Fig. 4. Comparison of Moment-Rotation Behavior by Experiment and Three-Parameter Power Model for Verification Study

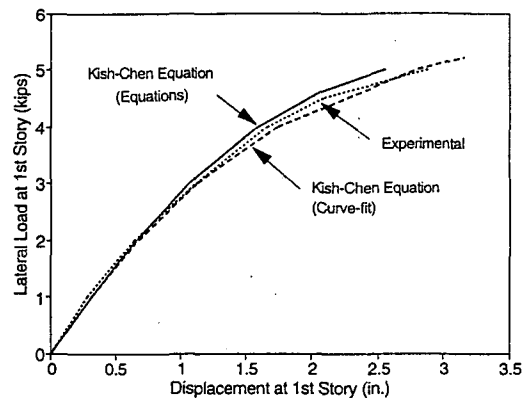


Fig. 5. Comparison of Lateral Displacements by Experiment and Proposed Methods for Verification Study

3.2 Effect of Geometric Imperfections

Chen and Kim performed a comprehensive verification study of various geometric imperfection effects on frame behavior by comparing the results of the proposed methods with those of the plastic-zone analysis and the conventional LRFD method [1]. Herein, some typical examples are presented in what follows.

The AISC-LRFD column strength curve is used here for a verification of the column strength since it properly accounts for the second-order effect, residual stresses, and geometric imperfections of an isolated column in a practical manner. In the explicit imperfection model, the two-element column is assumed to have an initial geometric imperfection equal to $L_c/1000$ at mid-height. The proposed model results in a good fit to the LRFD column strengths (Fig. 6).

Kanchanalai developed exact interaction curves using the plastic-zone analysis for sway frames [7]. In his study, the members were assumed to have maximum compressive residual stresses of $0.3F_y$ without geometric imperfections. Thus, the curves are adjusted here to account for geometric imperfections. The AISC-LRFD interaction curves are obtained based on the LeMessurier K-factor approach. The inelastic stiffness reduction factor τ is used with the

LeMessurier procedure for K-factor calculations. Geometric imperfection of $L_c/500$ is used. The proposed model predicts well the strengths of the frame (Fig. 7).

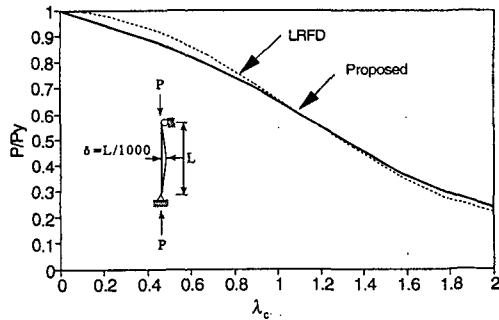


Fig. 6. Comparison of Strength Curves by Explicit Imperfection Modeling Method and LRFD Method for Axially Loaded Pin-Ended Column

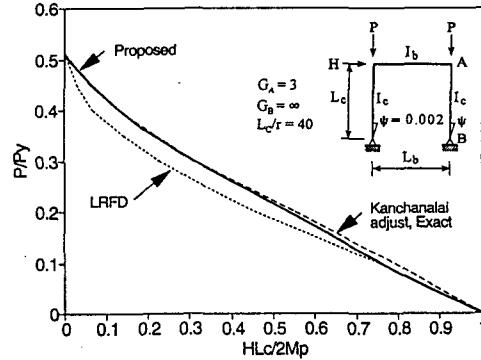


Fig. 7. Comparison of Strength Curves by Explicit Imperfection Modeling, Plastic-Zone, and LRFD Method for Portal Frame

4. DESIGN EXAMPLE

Figure 8 shows a two-story four-bay partially restrained frame. The height of each story is 12 feet and it is 25 feet wide. The spacing of the frames is 25 feet. The frame is subjected to a distributed gravity and concentrated lateral loads. The roof beams' connections are the top- and seat- $L6 \times 4.0 \times 3/8 \times 7$ angle with double web-angles of $L4 \times 3.5 \times 1/4 \times 5.5$ made of A36 steel. The floor beams' connections are the top- and seat-angles $L6 \times 4 \times 9/16 \times 7$ with double web-angles of $L4 \times 3.5 \times 5/16 \times 8.5$. All fasteners are A325 $3/4$ " Diameter bolts. All members are assumed to be continuously braced laterally. The load conditions are shown in Fig. 8.

The initial member sizes are selected as $W8 \times 21$, $W16 \times 40$, and $W12 \times 22$ for the columns, the floor beam, and the roof beam. Each column is modeled by one and the beams by two elements. The distributed gravity loads are converted to concentrated loads on the beam. The geometric imperfection is calculated by multiplying the column height by 0.002. The incremental loads are computed by dividing the concentrated load by the scaling factor of 20. The applied load increment is automatically reduced to minimize the error when the change in the element stiffness parameter ($\Delta\eta$) exceeds a defined tolerance. Using Eqs. in Ref. [1], the connection parameters are calculated as $R_{ki} = 90,877$ kip-in./rad., $M_u = 446$ kip-in, and $n = 1.403$ at roof level, and $R_{ki} = 607,384$ kip-in./rad., $M_u = 1,361$ kip-in, and $n = 0.927$ at floor level. The ultimate moments M_u are reduced by resistance factor of 0.9 (401 kip-in at roof level, 1,225 kip-in at floor level). The preliminary member sizes are satisfactory based on the analysis results.

For the design by the AISC-LRFD method, the initial member sizes are selected as $W8 \times 21$ exterior columns, $W8 \times 24$ interior columns, $W12 \times 19$ roof beams, and $W16 \times 36$ floor beams. The design may be performed by the procedure proposed by Barakat and Chen [8].

The member sizes by the proposed method and the LRFD method are compared in Fig. 9. The beam members are one size larger, and the interior columns are one size smaller in the proposed method.

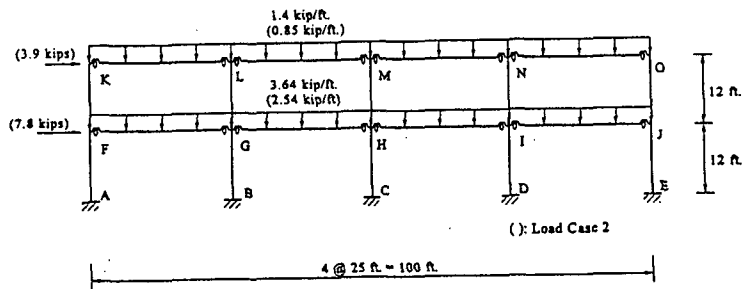


Fig. 8. Configuration of Two-Story Four-Bay Semi-Rigid Frame for Design Example

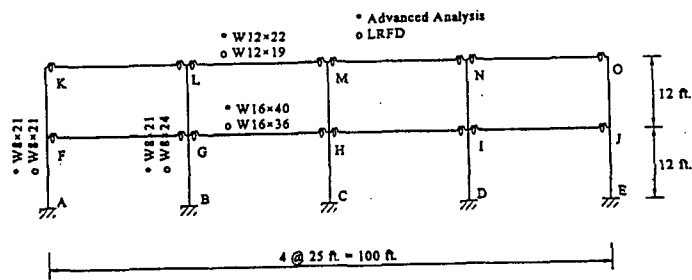


Fig. 9. Comparison of Member Sizes by Proposed Methods and LRFD Method for Design Example

5. CONCLUSIONS

An inelastic buckling analysis method is developed for partially restrained frame design. The strengths and displacements predicted by the method are compared well with those available experiments. Since the proposed method can predict accurately the combined effects of connection, geometric, and material nonlinearities for partially restrained frames in a direct manner, the method does not require separate member capacity checks including the calculations of K-factor. The proposed method provides a practical tool for the LRFD design of partially restrained frames. Since the proposed method strikes a balance between the requirement for realistic representation of actual behavior and failure mode of a structural system and the requirement for simplicity in use, it is therefore recommended for general use.

REFERENCES

1. Chen, W. F., and Kim, S. E., *LRFD Steel Design Using Advanced Analysis*, CRC Press (to be published in Feb. 1997)
2. American Institute of Steel Construction, *Load and Resistance Factor Design, Manual of Steel Construction*, Vol. 1 and 2, 2nd Ed., Chicago, Illinois, 1993.
3. Chen, W. F. and Lui, E. M., *Stability Design of Steel Frames*, CRC Press, 1991, 380pp.
4. Liew, J. Y. R., "Advanced Analysis for Frame Design," Ph.D. Thesis, School of Civil Engineering, Purdue University, West Lafayette, IN, 1992, 392 pp.
5. Kish, N. and Chen, W. F., "Moment-rotation Relations of Semi-rigid Connections with Angles," *Journal of Structural Engineering*, ASCE, 116, 7, 1990, pp. 1813-1834.
6. Stelmack T. W., "Analytical and Experimental Response of Flexibly-connected Steel Frames," M.S. Thesis, Department of Civil, Environmental, and Architectural Engineering, University of Colorado, 1982, 134 pp.
7. Kanchanalai, T., "The Design and Behavior of Beam-columns in Unbraced Steel Frames," *AISI Project No. 189, Report No. 2*, Civil Engineering/structures Research Lab., University of Texas, Austin, TX, 1977, 300pp.
8. Barakat, M. and Chen, W. F., "Practical Analysis of Semi-rigid Frames," *Engineering Journal*, AISC, Vol.27, No. 2, 1990, pp. 54-68.